

Contribution to the Theory of Planar Wire Loop Antennas Used for Reception

Frédéric Broyd^b, *Senior Member, IEEE*, and Evelyne Clavelier, *Senior Member, IEEE*

Abstract—Using “electromagnetic field” to designate an electric field and a magnetic field which satisfy Maxwell’s equations, we define a decomposition of an arbitrary incident time-harmonic electromagnetic field into four elementary time-harmonic electromagnetic fields \mathcal{F}_A , \mathcal{F}_B , \mathcal{F}_C , and \mathcal{F}_D . A formula, which gives the response of an arbitrary planar wire loop antenna used for reception, is based on this decomposition. This formula is applicable to any incident field configuration, and valid at any frequency at which the thin wire approximation applies. It separates the response of the antenna into three parts, one of which may be viewed as the intended response of the antenna. Our analysis teaches that \mathcal{F}_C and \mathcal{F}_D have no effect on the antenna and how \mathcal{F}_A and \mathcal{F}_B excite the antenna. Thus, it allows us to better understand the characteristics and limitations of a planar wire loop antenna used as a measuring antenna or as a direction finder.

Index Terms—Antenna theory, electrically small antenna, loop antenna, measuring antenna, receiving antenna.

I. INTRODUCTION

AN ELECTRICALLY small loop antenna may be used for measuring a magnetic component of an electromagnetic field [1]. For accurate measurements using a circular loop antenna, the feeder (i.e., feed line) of the antenna is often connected to the loop by utilizing a shielded-loop configuration, which prevents common-mode currents on the feeder from affecting the antenna’s response [2, Sec. 5-4] [3, Sec. 11.8]. The shield of a shielded-loop antenna operates like an unshielded loop antenna. Loop antennas are used for electromagnetic compatibility (EMC) testing in laboratories, and for various types of outdoor measurements such as site surveys, proof of performance of fixed antennas, propagation measurements, and spectrum monitoring [4, Sec. 13 Par. 41], [5]–[11]. Loop antennas that need not be electrically small are also used in direction-finding systems and high-frequency ground-wave radars [4, Sec. 12], [12]–[14].

According to a simplistic analysis, an open-circuit voltage at the port of an electrically small loop antenna used for reception is given by $j\omega S\mu_0 H_{NA}$, where ω is the radian frequency of an incident electromagnetic field and H_{NA} is the magnetic field normal to the plane of the loop, averaged over the surface S of the loop [2, Sec. 5-2]. A more elaborate analysis is available for electrically small single-turn square or circular

loop antennas subject to an incident plane wave having a real wave vector, which provides an approximate formula that includes a response of the loop antenna to the polarization for which H_{NA} is zero [1], [3, Sec. 11.7]. Unfortunately, this analysis only applies to an incident plane wave having a known real wave vector, or to several such waves if the formula is used repeatedly. Thus, it does not provide a general picture of what is sensed by the antenna if it is subject to an arbitrary incident electromagnetic field. For instance, it does not apply to the standard-field calibration technique, in which the circular loop antenna of a field-strength meter to be calibrated is excited by a coaxial circular loop placed at an electrically short distance [5]. For instance, it does not apply to measurement configurations in which a planar loop antenna used for measurements lies in the near-field of a device under test. For instance, it does not apply to outdoor measurements where multiple sources at unknown locations contribute to the measured signal.

Broadly speaking, the purpose of this paper is to investigate some general properties of a planar wire loop antenna (which need neither be electrically small, nor circular) used for receiving an incident electromagnetic field (which need not be a uniform plane wave), to better understand its characteristics and limitations as a measuring antenna or as a direction finder. We shall use “electromagnetic field” to designate the ordered pair $\mathcal{F} = (\mathbf{E}, \mathbf{H})$ of an electric field \mathbf{E} and a magnetic field \mathbf{H} which satisfy Maxwell’s equations in a specified region. The main new results of this paper are:

- a simple decomposition of an arbitrary incident time-harmonic electromagnetic field into 4 elementary time-harmonic electromagnetic fields (ETHEFs), defined in Section III, which is relevant to better understand the operation of planar wire loop antennas; and
- an exact formula, obtained in Section IV, which is based on the ETHEF decomposition and which provides the open-circuit voltage at the port of a planar wire loop antenna having any shape, structure and size, subject to an arbitrary incident time-harmonic electromagnetic field.

The ETHEF decomposition is applied to different incident electromagnetic fields, in Sections V and VI.

II. ASSUMPTIONS AND KNOWN RESULTS

A. Assumptions About the Loop Antenna

We use the traditional rectangular coordinate system $Oxyz$, of unit vectors \mathbf{u}_x , \mathbf{u}_y , and \mathbf{u}_z . We use “planar wire loop antenna” to designate an antenna made of a single thin wire lying in the plane $z = 0$. This thin wire forms a curve, the ends

Manuscript received June 5, 2019; revised September 6, 2019; accepted September 25, 2019. Date of publication October 28, 2019; date of current version March 3, 2020. (Corresponding author: Frédéric Broyd.)

The authors are with Excem, 78580 Maule, France (e-mail: fredbroyde@excem.fr; eclavelier@excem.fr).

Color versions of one or more of the figures in this article are available online at <http://ieeexplore.ieee.org>.

Digital Object Identifier 10.1109/TAP.2019.2948568

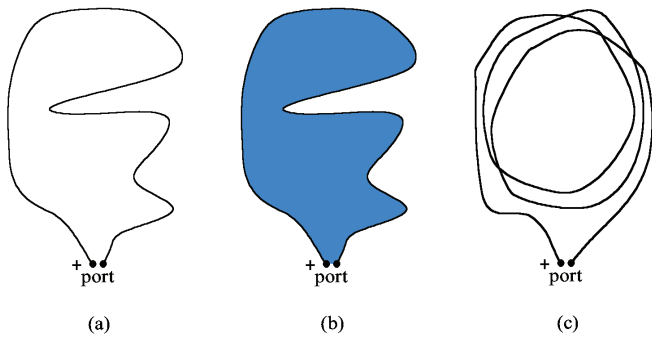


Fig. 1. A non-self-intersecting planar loop antenna (a), the surface inside the single loop formed by this antenna and the arbitrary path over the gap (b), and a self-intersecting planar loop antenna (c).

of which are connected to the terminals of the antenna port, which lie in the plane $z = 0$. The physical space between these terminals is the gap. An arbitrary path over the gap, which is assumed to lie in the plane $z = 0$, is added to this curve, to obtain a closed path.

A front view of a non-self-intersecting planar loop antenna is shown in Fig. 1(a). For this type of loop antenna, the thin wire and the arbitrary path over the gap form a non-self-intersecting continuous loop in the plane $z = 0$, which bounds the surface shown in Fig. 1(b).

A front view of a self-intersecting planar loop antenna is shown in Fig. 1(c). We assume that there is no electric contact at the crossing points which appear in the front view. This implies that, at such a crossing point, the crossing arcs of the wire are separated in the z direction. Thus, the antenna is not strictly planar, but we nevertheless assume that the extent of the loop antenna in the z direction is so small that it may be ignored in our computations. For this type of loop antenna, the thin wire and the arbitrary path over the gap have multiple turns. We will see in Section IV how we can count the turns and identify the corresponding loops.

B. Reception by a Thin Wire Antenna

For any wire antenna, the open circuit voltage e_{ant} of the antenna used for reception is given by

$$e_{ant} = -\frac{1}{I_0} \iiint_{\text{Antenna}} \mathbf{J}_t \cdot \mathbf{E}_i dv \quad (1)$$

where \mathbf{J}_t is the current density in the antenna if it is used for emission and a current I_0 flows into the positive terminal of the antenna port, where \mathbf{E}_i is the incident electric field, and where dv is a volume element [15, Sec. 13.06]. It must be emphasized that this formula is exact, since it is only based on reciprocity. In the case of a thin-wire antenna along which a curvilinear abscissa s is defined, we obtain

$$e_{ant} = -\int_{\text{Antenna}} \frac{i(s)}{I_0} \mathbf{u}_t \cdot \mathbf{E}_i(s) ds \quad (2)$$

where $i(s)$ is the current in the thin wire if the antenna is used for emission and a current I_0 flows into the positive terminal of the antenna port, where \mathbf{u}_t is a unit vector tangent to the thin wire, its direction being the direction of positive current,

where $\mathbf{E}_i(s)$ is the incident electric field, and where ds is the length element.

C. TE and TM Components

We consider an arbitrary incident time-harmonic electromagnetic field $\mathcal{F}_i = (\mathbf{E}_i, \mathbf{H}_i)$, in an homogeneous and source-free region characterized by the complex permittivity ϵ and the complex permeability μ , so that $k = \omega(\epsilon\mu)^{1/2}$, where the power 1/2 means the principal square root. It is well known that \mathcal{F}_i can be expressed as the sum of two components: an electromagnetic field $\mathcal{F}_{TM} = (\mathbf{E}_{TM}, \mathbf{H}_{TM})$ transverse magnetic (TM) to z ; and an electromagnetic field $\mathcal{F}_{TE} = (\mathbf{E}_{TE}, \mathbf{H}_{TE})$ transverse electric (TE) to z [16, Ch. 13], [17, Sec. 3.12]. For \mathcal{F}_{TM} , we have

$$\mathbf{H}_{TM} = \nabla \times (\psi_{TM} \mathbf{u}_z) = \nabla \psi_{TM} \times \mathbf{u}_z \quad (3)$$

and

$$\mathbf{E}_{TM} = \frac{1}{j\omega\epsilon} \nabla \times \nabla \times (\psi_{TM} \mathbf{u}_z) \quad (4)$$

where the scalar distribution ψ_{TM} has the dimensions of current and satisfies the Helmholtz equation

$$\nabla^2 \psi_{TM} + k^2 \psi_{TM} = 0. \quad (5)$$

Let us use E_{TMx} , E_{TM_y} , and E_{TMz} to denote the rectangular coordinates of \mathbf{E}_{TM} , and H_{TMx} , H_{TM_y} , and H_{TMz} to denote the rectangular coordinates of \mathbf{H}_{TM} . We have

$$E_{TMx} = \frac{1}{j\omega\epsilon} \frac{\partial^2 \psi_{TM}}{\partial x \partial z} \quad (6)$$

$$E_{TM_y} = \frac{1}{j\omega\epsilon} \frac{\partial^2 \psi_{TM}}{\partial y \partial z} \quad (7)$$

$$\begin{aligned} E_{TMz} &= -\frac{1}{j\omega\epsilon} \left(\frac{\partial^2 \psi_{TM}}{\partial x^2} + \frac{\partial^2 \psi_{TM}}{\partial y^2} \right) \\ &= \frac{1}{j\omega\epsilon} \left(\frac{\partial^2 \psi_{TM}}{\partial z^2} + k^2 \psi_{TM} \right) \end{aligned} \quad (8)$$

$$H_{TMx} = \frac{\partial \psi_{TM}}{\partial y} \quad (9)$$

$$H_{TM_y} = -\frac{\partial \psi_{TM}}{\partial x} \quad (10)$$

and

$$H_{TMz} = 0. \quad (11)$$

For \mathcal{F}_{TE} , we have

$$\mathbf{E}_{TE} = -\nabla \times (\psi_{TE} \mathbf{u}_z) = -\nabla \psi_{TE} \times \mathbf{u}_z \quad (12)$$

and

$$\mathbf{H}_{TE} = \frac{1}{j\omega\mu} \nabla \times \nabla \times (\psi_{TE} \mathbf{u}_z) \quad (13)$$

where the scalar distribution ψ_{TE} has the dimensions of voltage and satisfies the Helmholtz equation

$$\nabla^2 \psi_{TE} + k^2 \psi_{TE} = 0. \quad (14)$$

Let us use E_{TE_x} , E_{TE_y} , and E_{TE_z} to denote the rectangular coordinates of \mathbf{E}_{TE} , and H_{TE_x} , H_{TE_y} , and H_{TE_z} to denote the rectangular coordinates of \mathbf{H}_{TE} . We have

$$E_{TE_x} = -\frac{\partial \psi_{TE}}{\partial y} \quad (15)$$

$$E_{TE_y} = \frac{\partial \psi_{TE}}{\partial x} \quad (16)$$

$$E_{TE_z} = 0 \quad (17)$$

$$H_{TE_x} = \frac{1}{j\omega\mu} \frac{\partial^2 \psi_{TE}}{\partial x \partial z} \quad (18)$$

$$H_{TE_y} = \frac{1}{j\omega\mu} \frac{\partial^2 \psi_{TE}}{\partial y \partial z} \quad (19)$$

and

$$\begin{aligned} H_{TE_z} &= -\frac{1}{j\omega\mu} \left(\frac{\partial^2 \psi_{TE}}{\partial x^2} + \frac{\partial^2 \psi_{TE}}{\partial y^2} \right) \\ &= \frac{1}{j\omega\mu} \left(\frac{\partial^2 \psi_{TE}}{\partial z^2} + k^2 \psi_{TE} \right). \end{aligned} \quad (20)$$

Let \mathbf{E}_i and \mathbf{H}_i be the electric field and the magnetic field of \mathcal{F}_i , respectively. Since, as explained above,

$$\mathcal{F}_i = \mathcal{F}_{TE} + \mathcal{F}_{TM} \quad (21)$$

it follows from (8) and (17) that the distribution ψ_{TM} satisfies

$$\frac{\partial^2 \psi_{TM}}{\partial z^2} + k^2 \psi_{TM} = j\omega\epsilon E_{iz} \quad (22)$$

which can be used to determine ψ_{TM} if $E_{iz} = \mathbf{E}_i \cdot \mathbf{u}_z$ is known, and it follows from (11) and (20) that the distribution ψ_{TE} satisfies

$$\frac{\partial^2 \psi_{TE}}{\partial z^2} + k^2 \psi_{TE} = j\omega\mu H_{iz} \quad (23)$$

which can be used to determine ψ_{TE} if $H_{iz} = \mathbf{H}_i \cdot \mathbf{u}_z$ is known.

The existence of a decomposition of \mathcal{F}_i into a TM component (the electromagnetic field \mathcal{F}_{TM}) and a TE component (the electromagnetic field \mathcal{F}_{TE}) does not entail that this decomposition is unique. This is caused by the fact that \mathcal{F}_i may comprise an electromagnetic field which is both TE to z and TM to z , which may therefore be either a part of \mathcal{F}_{TM} or a part of \mathcal{F}_{TE} [18, Sec. 10.3]. We will use this observation in the definition of ψ_{TE} in Section V.

III. THE ETHEFS OF AN INCIDENT ELECTROMAGNETIC FIELD

A. Mirror-Symmetric and Mirror-Antisymmetric Parts

We consider an arbitrary incident time-harmonic electromagnetic field \mathcal{F}_i , in a region which includes a part of the plane $z = 0$. Let \mathcal{F}_m be the result of the transformation of \mathcal{F}_i under reflection in the plane $z = 0$. Let $\mathbf{E}_i(x, y, z)$ and $\mathbf{H}_i(x, y, z)$ be the electric field and the magnetic field of \mathcal{F}_i , respectively, at a point of rectangular coordinates (x, y, z) ; and $\mathbf{E}_m(x, y, z)$ and $\mathbf{H}_m(x, y, z)$ be the electric field and the magnetic field of \mathcal{F}_m , respectively, at this point. We know that \mathcal{F}_m is an electromagnetic field which satisfies [19, Sec. 6.11]:

$$\mathbf{E}_m(x, y, -z) = \mathbf{E}_i(x, y, z) - 2(\mathbf{E}_i(x, y, z) \cdot \mathbf{u}_z)\mathbf{u}_z \quad (24)$$

and

$$\mathbf{H}_m(x, y, -z) = -[\mathbf{H}_i(x, y, z) - 2(\mathbf{H}_i(x, y, z) \cdot \mathbf{u}_z)\mathbf{u}_z] \quad (25)$$

Let us use $E_{ix}(x, y, z)$, $E_{iy}(x, y, z)$, and $E_{iz}(x, y, z)$ to denote the rectangular coordinates of $\mathbf{E}_i(x, y, z)$; $E_{mx}(x, y, z)$, $E_{my}(x, y, z)$, and $E_{mz}(x, y, z)$ the rectangular coordinates of $\mathbf{E}_m(x, y, z)$; $H_{ix}(x, y, z)$, $H_{iy}(x, y, z)$, and $H_{iz}(x, y, z)$ the rectangular coordinates of $\mathbf{H}_i(x, y, z)$; and $H_{mx}(x, y, z)$, $H_{my}(x, y, z)$, and $H_{mz}(x, y, z)$ the rectangular coordinates of $\mathbf{H}_m(x, y, z)$. Eq. (24) and (25) are equivalent to

$$E_{mx}(x, y, -z) = E_{ix}(x, y, z) \quad (26)$$

$$E_{my}(x, y, -z) = E_{iy}(x, y, z) \quad (27)$$

$$E_{mz}(x, y, -z) = -E_{iz}(x, y, z) \quad (28)$$

$$H_{mx}(x, y, -z) = -H_{ix}(x, y, z) \quad (29)$$

$$H_{my}(x, y, -z) = -H_{iy}(x, y, z) \quad (30)$$

and

$$H_{mz}(x, y, -z) = H_{iz}(x, y, z). \quad (31)$$

We can now define the mirror-symmetric part of \mathcal{F}_i as

$$\mathcal{F}_{MS} = \frac{\mathcal{F}_i + \mathcal{F}_m}{2} \quad (32)$$

and the mirror-antisymmetric part of \mathcal{F}_i as

$$\mathcal{F}_{AS} = \frac{\mathcal{F}_i - \mathcal{F}_m}{2}. \quad (33)$$

Being linear combinations of electromagnetic fields, \mathcal{F}_{MS} and \mathcal{F}_{AS} are electromagnetic fields. Since

$$\mathcal{F}_i = \mathcal{F}_{MS} + \mathcal{F}_{AS} \quad (34)$$

we have obtained a decomposition of \mathcal{F}_i into two electromagnetic fields.

Let us use $\mathbf{E}_{MS}(x, y, z)$ and $\mathbf{H}_{MS}(x, y, z)$ to denote the electric field and the magnetic field of \mathcal{F}_{MS} , respectively, at a point of rectangular coordinates (x, y, z) . Let us use $E_{MSx}(x, y, z)$, $E_{MSy}(x, y, z)$, and $E_{MSz}(x, y, z)$ to denote the rectangular coordinates of $\mathbf{E}_{MS}(x, y, z)$; and $H_{MSx}(x, y, z)$, $H_{MSy}(x, y, z)$, and $H_{MSz}(x, y, z)$ to denote the rectangular coordinates of $\mathbf{H}_{MS}(x, y, z)$. By (26)–(32), we have

$$E_{MSx}(x, y, 0) = E_{ix}(x, y, 0) \quad (35)$$

$$E_{MSy}(x, y, 0) = E_{iy}(x, y, 0) \quad (36)$$

$$E_{MSz}(x, y, 0) = 0 \quad (37)$$

$$H_{MSx}(x, y, 0) = H_{MSy}(x, y, 0) = 0 \quad (38)$$

and

$$H_{MSz}(x, y, 0) = H_{iz}(x, y, 0). \quad (39)$$

Let us use $\mathbf{E}_{AS}(x, y, z)$ and $\mathbf{H}_{AS}(x, y, z)$ to denote the electric field and the magnetic field of \mathcal{F}_{AS} , respectively, at a point of rectangular coordinates (x, y, z) . Let us use $E_{ASx}(x, y, z)$, $E_{ASy}(x, y, z)$, and $E_{ASz}(x, y, z)$ to denote the rectangular coordinates of $\mathbf{E}_{AS}(x, y, z)$; and $H_{ASx}(x, y, z)$,

$H_{ASy}(x, y, z)$, and $H_{ASz}(x, y, z)$ to denote the rectangular coordinates of $\mathbf{H}_{AS}(x, y, z)$. By (26)–(31) and (33), we have

$$E_{ASx}(x, y, 0) = E_{ASy}(x, y, 0) = 0 \quad (40)$$

$$E_{ASz}(x, y, 0) = E_{iz}(x, y, 0) \quad (41)$$

$$H_{ASx}(x, y, 0) = H_{ix}(x, y, 0) \quad (42)$$

$$H_{ASy}(x, y, 0) = H_{iy}(x, y, 0) \quad (43)$$

and

$$H_{ASz}(x, y, 0) = 0. \quad (44)$$

B. Definition of the ETHEFs

We consider an arbitrary incident time-harmonic electromagnetic field \mathcal{F}_i , in an homogeneous and source-free region which includes a part of the plane $z = 0$, and which is characterized by the complex permittivity ϵ , and the complex permeability μ . For an arbitrary vector \mathbf{v} , we use v_z to denote $\mathbf{v} \cdot \mathbf{u}_z$, and \mathbf{v}_\perp to denote the vector

$$\mathbf{v}_\perp = \mathbf{v} - (\mathbf{v} \cdot \mathbf{u}_z)\mathbf{u}_z = (\mathbf{v} \cdot \mathbf{u}_x)\mathbf{u}_x + (\mathbf{v} \cdot \mathbf{u}_y)\mathbf{u}_y. \quad (45)$$

Likewise, we introduce the operator ∇_\perp which, in cartesian form, is

$$\nabla_\perp = \mathbf{u}_x \frac{\partial}{\partial x} + \mathbf{u}_y \frac{\partial}{\partial y} \quad (46)$$

so that

$$\nabla_\perp^2 = \frac{\partial^2}{\partial x^2} + \frac{\partial^2}{\partial y^2}. \quad (47)$$

We first apply the TM/TE decomposition, to obtain \mathcal{F}_{TM} and \mathcal{F}_{TE} . By (3) and (6)–(11), \mathcal{F}_{TM} is given by:

$$\mathbf{E}_{TM\perp} = \frac{1}{j\omega\epsilon} \frac{\partial}{\partial z} \nabla_\perp \psi_{TM} \quad (48)$$

$$E_{TMz} = -\frac{1}{j\omega\epsilon} \nabla_\perp^2 \psi_{TM} \quad (49)$$

$$\mathbf{H}_{TM\perp} = \nabla \psi_{TM} \times \mathbf{u}_z = \nabla_\perp \psi_{TM} \times \mathbf{u}_z \quad (50)$$

and

$$H_{TMz} = 0. \quad (51)$$

By (12) and (15)–(20), \mathcal{F}_{TE} is given by:

$$\mathbf{E}_{TE\perp} = -\nabla \psi_{TE} \times \mathbf{u}_z = -\nabla_\perp \psi_{TE} \times \mathbf{u}_z \quad (52)$$

$$E_{TEz} = 0 \quad (53)$$

$$\mathbf{H}_{TE\perp} = \frac{1}{j\omega\mu} \frac{\partial}{\partial z} \nabla_\perp \psi_{TE} \quad (54)$$

and

$$H_{TEz} = -\frac{1}{j\omega\mu} \nabla_\perp^2 \psi_{TE}. \quad (55)$$

We define the four ETHEFs of \mathcal{F}_i as follows:

- the first ETHEF is the mirror-symmetric part of \mathcal{F}_{TE} , denoted by $\mathcal{F}_A = (\mathbf{E}_A, \mathbf{H}_A)$;
- the second ETHEF is the mirror-symmetric part of \mathcal{F}_{TM} , denoted by $\mathcal{F}_B = (\mathbf{E}_B, \mathbf{H}_B)$;
- the third ETHEF is the mirror-antisymmetric part of \mathcal{F}_{TE} , denoted by $\mathcal{F}_C = (\mathbf{E}_C, \mathbf{H}_C)$; and

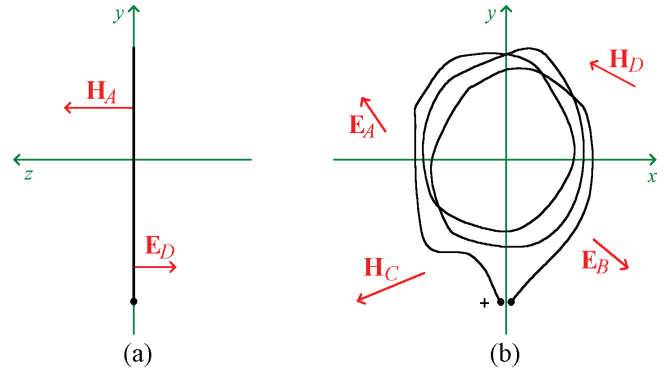


Fig. 2. The planar loop antenna of Fig. 1(c), and the nonzero vectors given by (57)–(64), each represented at an arbitrary observation point in the plane $z = 0$, as if it was a real vector having the dimensions of length. The vectors which are orthogonal to the plane $z = 0$ are shown in the right side view of the loop antenna (a). The vectors which lie in the plane $z = 0$ are shown in the front view of the loop antenna (b).

- the fourth ETHEF is the mirror-antisymmetric part of \mathcal{F}_{TM} , denoted by $\mathcal{F}_D = (\mathbf{E}_D, \mathbf{H}_D)$.

By (21) and (34), we have

$$\mathcal{F}_i = \mathcal{F}_A + \mathcal{F}_B + \mathcal{F}_D + \mathcal{F}_C \quad (56)$$

which provides a decomposition of \mathcal{F}_i into four components, each of which could exist independently of the others.

By (35)–(44) and (48)–(55), in the plane $z = 0$, we have

$$\mathbf{E}_A = -\nabla_\perp \psi_{TE} \times \mathbf{u}_z \quad (57)$$

$$\mathbf{H}_A = -\frac{\mathbf{u}_z}{j\omega\mu} \nabla_\perp^2 \psi_{TE} \quad (58)$$

$$\mathbf{E}_B = \frac{1}{j\omega\epsilon} \frac{\partial}{\partial z} \nabla_\perp \psi_{TM} \quad (59)$$

$$\mathbf{H}_B = \mathbf{0} \quad (60)$$

$$\mathbf{E}_C = \mathbf{0} \quad (61)$$

$$\mathbf{H}_C = \frac{1}{j\omega\mu} \frac{\partial}{\partial z} \nabla_\perp \psi_{TE} \quad (62)$$

$$\mathbf{E}_D = -\frac{\mathbf{u}_z}{j\omega\epsilon} \nabla_\perp^2 \psi_{TM} \quad (63)$$

and

$$\mathbf{H}_D = \nabla_\perp \psi_{TM} \times \mathbf{u}_z. \quad (64)$$

Since $\nabla_\perp \psi_{TM}$ and $\nabla_\perp \psi_{TE}$ are normal to \mathbf{u}_z , it follows that, in the plane $z = 0$:

- \mathcal{F}_A has a magnetic field which is normal to this plane, whereas \mathcal{F}_B , \mathcal{F}_C , and \mathcal{F}_D have each a magnetic field which is parallel to this plane, or a null vector; and
- \mathcal{F}_A and \mathcal{F}_B each have an electric field which is parallel to this plane, whereas \mathcal{F}_C and \mathcal{F}_D have each an electric field which is normal to this plane, or a null vector.

The vectors given by (57)–(64) are represented in Fig. 2. Using (56)–(64), we find that, in the plane $z = 0$,

$$\mathbf{H}_A = (\mathbf{H}_i \cdot \mathbf{u}_z)\mathbf{u}_z \quad (65)$$

and

$$\mathbf{E}_D = (\mathbf{E}_i \cdot \mathbf{u}_z)\mathbf{u}_z. \quad (66)$$

Thus, even though \mathcal{F}_{TM} and \mathcal{F}_{TE} need not be uniquely defined, \mathbf{H}_A , \mathbf{H}_B , \mathbf{E}_C and \mathbf{E}_D are uniquely defined in the plane $z = 0$. Also, $\mathbf{E}_A + \mathbf{E}_B$ and $\mathbf{H}_C + \mathbf{H}_D$ are uniquely defined everywhere, because they are the electric field of the mirror-symmetric part of \mathcal{F}_i , and the magnetic field of the mirror-antisymmetric part of \mathcal{F}_i , respectively.

IV. RESPONSE OF A PLANAR LOOP ANTENNA OF ANY SHAPE AND SIZE

By (2) and (56), the open-circuit voltage of the planar wire loop antenna of Section II-A, used for reception of the incident time-harmonic electromagnetic field \mathcal{F}_i , is given by

$$e_{ant} = - \oint \frac{i(s)}{I_0} \mathbf{u}_t \cdot (\mathbf{E}_A + \mathbf{E}_B + \mathbf{E}_C + \mathbf{E}_D) ds \quad (67)$$

where the integration path is closed by the arbitrary path over the gap, in which $i(s) = 0$. For reasons which will become apparent later, the arbitrary path over the gap should be as short as possible, for instance a straight line, but this is not required. The positive orientation of the integration path, which corresponds to the orientation of \mathbf{u}_t , goes from the positive terminal of the antenna port to the negative terminal of the antenna port along the thin wire, and then from the negative terminal to the positive terminal along the arbitrary path over the gap. Using (61) and (63), we get

$$e_{ant} = - \oint \frac{I_0 + (i(s) - I_0)}{I_0} \mathbf{u}_t \cdot (\mathbf{E}_A + \mathbf{E}_B) ds. \quad (68)$$

\mathcal{F}_A and \mathcal{F}_B being electromagnetic fields, we have $\nabla \times \mathbf{E}_A = -j\omega\mu\mathbf{H}_A$ and $\nabla \times \mathbf{E}_B = -j\omega\mu\mathbf{H}_B$. Thus, if the integration path has a single turn, we have

$$\oint \mathbf{u}_t \cdot (\mathbf{E}_A + \mathbf{E}_B) ds = -j\omega\mu\kappa \iint_S (\mathbf{H}_A + \mathbf{H}_B) \cdot \mathbf{u}_z da \quad (69)$$

where $\kappa = 1$ if the orientation of the integration path agrees with the orientation \mathbf{u}_z of the surface-element da of the plane $z = 0$, and $\kappa = -1$ in the opposite case. The assumption ‘‘the integration path has a single turn’’ means that the integration path forms a non-self-intersecting continuous loop in the plane $z = 0$. It entails that the line integral of the left-hand side of (69) is, according to Stoke’s theorem, equal to a surface integral over the part of the plane $z = 0$ which is bounded by the integration path, this part being denoted by \mathcal{S} in (69). By (60), we have

$$\oint \mathbf{u}_t \cdot (\mathbf{E}_A + \mathbf{E}_B) ds = -j\omega\mu\kappa \iint_S \mathbf{H}_A \cdot \mathbf{u}_z da. \quad (70)$$

If the integration path forms a self-intersecting continuous loop in the plane $z = 0$, we use the following algorithm: (step 1) we start from the positive terminal of the antenna port and set the turn index n to 0; (step 2) moving along the integration path in the positive direction, as soon as a loop is formed with the part of the integration path already traveled and not erased, n is incremented by 1, the value κ_n of κ for this loop n is determined as explained above, and the line integral over loop n is, using Stoke’s theorem, replaced with a surface integral over the part of the plane $z = 0$ which is bounded by loop n ,

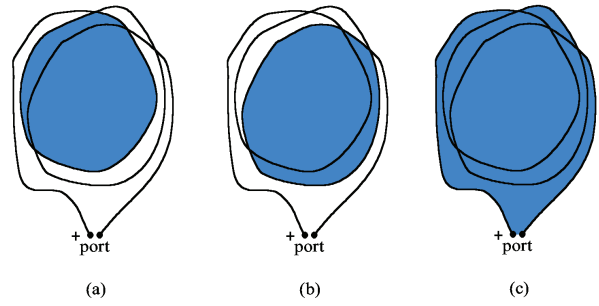


Fig. 3. The planar loop antenna of Fig. 1(c), and the 3 surfaces bounded by a loop obtained using the proposed algorithm.

this part being denoted by $\mathcal{S}(n)$; (step 3) this loop is erased from the integration path for the rest of the algorithm; (step 4) if the end of the integration path is not reached, we go back to step 2, otherwise we go to step 5; and (step 5) we set the number of turns, denoted by N , to n and end the algorithm.

For the planar loop antenna of Fig. 1(c), an implementation of this algorithm is represented in Fig. 3, in which (a) shows $\mathcal{S}(1)$; (b) shows $\mathcal{S}(2)$; and (c) shows $\mathcal{S}(3)$. In this example, we have $N = 3$ and $\kappa_1 = \kappa_2 = \kappa_3$. Using Fig. 2(b), we find $\kappa_1 = \kappa_2 = \kappa_3 = -1$. We note that the algorithm would not work if the antenna was not planar. The algorithm leads us to the general result

$$\oint \mathbf{u}_t \cdot (\mathbf{E}_A + \mathbf{E}_B) ds = -j\omega\mu \sum_{n=1}^N \kappa_n \iint_{\mathcal{S}(n)} \mathbf{H}_A \cdot \mathbf{u}_z da. \quad (71)$$

Using (71) in (68), we obtain

$$e_{ant} = j\omega\mu \sum_{n=1}^N \kappa_n \iint_{\mathcal{S}(n)} \mathbf{H}_A \cdot \mathbf{u}_z da - \oint \frac{i(s) - I_0}{I_0} \mathbf{u}_t \cdot (\mathbf{E}_A + \mathbf{E}_B) ds \quad (72)$$

which, for a single loop or identical loops, becomes

$$e_{ant} = j\omega\mu N\kappa \iint_S \mathbf{H}_A \cdot \mathbf{u}_z da - \oint \frac{i(s) - I_0}{I_0} \mathbf{u}_t \cdot (\mathbf{E}_A + \mathbf{E}_B) ds. \quad (73)$$

In (72) and (73), the line integral is zero if $i(s)$ is uniform in the thin wire and if the length of the arbitrary path over the gap is zero. It may therefore be ignored if the frequency is sufficiently low to allow us to consider that $i(s) = I_0$ everywhere in the thin wire, and if the length of the arbitrary path over the gap is sufficiently short. This is why the arbitrary path over the gap should be as short as possible. As said in Section III, \mathbf{H}_A and $\mathbf{E}_A + \mathbf{E}_B$ are uniquely defined in the plane $z = 0$, so that (72) and (73) are uniquely defined. In (72) and (73), the contributions of \mathbf{H}_A and \mathbf{E}_A are related because they correspond to the effect of \mathcal{F}_A , determined by ψ_{TE} , whereas the contribution of \mathbf{E}_B , which corresponds to the effect of \mathcal{F}_B , determined by ψ_{TM} , is completely independent from the contributions of \mathbf{H}_A and \mathbf{E}_A .

The decomposition of \mathcal{F}_i into four ETHEFs is particularly relevant to planar wire loop antennas which are intended to, or

expected to, be mainly responsive to a magnetic field orthogonal to the plane of the antenna (such as most electrically small planar wire loop antennas), since, in this context:

- the ETHEF \mathcal{F}_A causes the intended or expected response of the antenna;
- the ETHEF \mathcal{F}_B may cause an unwanted or unexpected response of the antenna; and
- the ETHEFs \mathcal{F}_C and \mathcal{F}_D cannot cause any response of the antenna.

The use of \mathbf{H}_A , \mathbf{E}_A , and \mathbf{E}_B in (72) and (73) shows how \mathcal{F}_A and \mathcal{F}_B excite the antenna. However, computing \mathbf{H}_A , \mathbf{E}_A , and \mathbf{E}_B is not required to obtain e_{ant} , since, by (56)–(64), we also have

$$e_{ant} = j\omega\mu \sum_{n=1}^N \kappa_n \iint_{S(n)} \mathbf{H}_{TE} \cdot \mathbf{u}_z da - \oint \frac{i(s) - I_0}{I_0} \mathbf{u}_t \cdot (\mathbf{E}_{TE} + \mathbf{E}_{TM}) ds \quad (74)$$

if we use the decomposition of \mathcal{F}_i into \mathcal{F}_{TE} and \mathcal{F}_{TM} , and

$$e_{ant} = j\omega\mu \sum_{n=1}^N \kappa_n \iint_{S(n)} \mathbf{H}_i \cdot \mathbf{u}_z da - \oint \frac{i(s) - I_0}{I_0} \mathbf{u}_t \cdot \mathbf{E}_i ds \quad (75)$$

if we use no decomposition of \mathcal{F}_i . If \mathbf{H}_A , \mathbf{E}_A , and \mathbf{E}_B are not known, (74) or (75) may be easier to compute than (73). However, they require information that is not needed to determine e_{ant} , because, at $z = 0$, \mathbf{H}_i , and \mathbf{E}_i contain more information about \mathcal{F}_i than \mathbf{H}_{TE} , \mathbf{E}_{TE} , and \mathbf{E}_{TM} , which contain more information about \mathcal{F}_i than \mathbf{H}_A , \mathbf{E}_A , and \mathbf{E}_B , the unnecessary information being ignored in (74) and (75).

V. APPLICATION TO AN INCIDENT PLANE WAVE

Let $\mathbf{k}_i = k_{ix}\mathbf{u}_x + k_{iy}\mathbf{u}_y + k_{iz}\mathbf{u}_z$ be an arbitrary complex wave vector such that

$$\mathbf{k}_i \cdot \mathbf{k}_i = k^2 = \omega^2\epsilon\mu. \quad (76)$$

Let i_{TM} be an arbitrary complex number having the dimensions of current, v_{TM} be an arbitrary complex number having the dimensions of voltage, and \mathbf{e}_{TEM} be an arbitrary complex vector having the dimensions of electric field and such that $\mathbf{e}_{TEM} \cdot \mathbf{u}_z = 0$. Here, i_{TM} , v_{TM} , and \mathbf{e}_{TEM} are independent of the observation point. The radius vector of the observation point being denoted by \mathbf{r} , we posit

$$\psi_{TM} = i_{TM} e^{-j\mathbf{k}_i \cdot \mathbf{r}} \quad (77)$$

so that (5) is satisfied. We posit

$$\psi_{TE} = \begin{cases} (\mathbf{e}_{TEM} \times \mathbf{u}_z) \cdot \mathbf{r} e^{-j\mathbf{k}_i \cdot \mathbf{r}}, & \text{if } k_{ix} = k_{iy} = 0 \\ v_{TE} e^{-j\mathbf{k}_i \cdot \mathbf{r}}, & \text{else} \end{cases} \quad (78)$$

so that (14) is satisfied in both cases. The first case of (78) corresponds to a wave which is TE to z and TM to z (i.e., TEM to z), arbitrarily considered as a TE wave.

Here, \mathcal{F}_i is a general time-harmonic plane wave in an homogeneous and source-free region characterized by the complex permittivity ϵ and the complex permeability μ . It

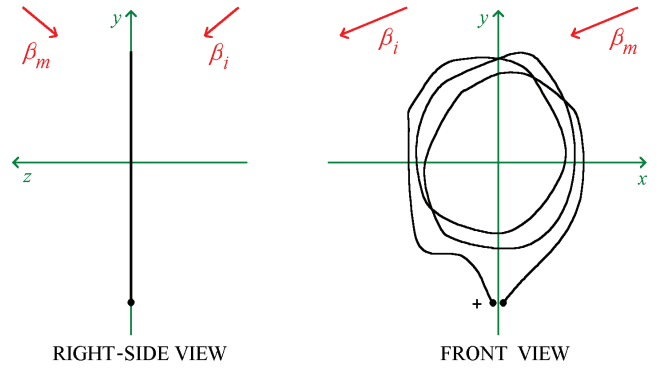


Fig. 4. The planar loop antenna of Fig. 1(c), and the vectors β_i and β_m , each represented at an arbitrary observation point in space, as if they had the dimensions of length. They are independent of the observation point.

is discussed in [17, Sec 2.11] and [17, Sec 4.2], where it is explained that the real part of \mathbf{k}_i indicates the direction of propagation. Let $k_{iz} = \mathbf{k}_i \cdot \mathbf{u}_z$ and $\mathbf{k}_{i\perp}$ be the vector defined by letting $\mathbf{v} = \mathbf{k}_i$ in (45). Using (48)–(55), we find that the TE and TM components of \mathcal{F}_i are, if $\mathbf{k}_{i\perp} \neq \mathbf{0}$, given by

$$\mathbf{E}_{TE} = jv_{TE} \mathbf{k}_{i\perp} \times \mathbf{u}_z e^{-j\mathbf{k}_i \cdot \mathbf{r}} \quad (79)$$

$$\mathbf{H}_{TE} = \frac{v_{TE}}{j\omega\mu} [(\mathbf{k}_{i\perp} \cdot \mathbf{k}_{i\perp})\mathbf{u}_z - k_{iz}\mathbf{k}_{i\perp}] e^{-j\mathbf{k}_i \cdot \mathbf{r}} \quad (80)$$

$$\mathbf{E}_{TM} = \frac{i_{TM}}{j\omega\epsilon} [(\mathbf{k}_{i\perp} \cdot \mathbf{k}_{i\perp})\mathbf{u}_z - k_{iz}\mathbf{k}_{i\perp}] e^{-j\mathbf{k}_i \cdot \mathbf{r}} \quad (81)$$

and

$$\mathbf{H}_{TM} = -ji_{TM} \mathbf{k}_{i\perp} \times \mathbf{u}_z e^{-j\mathbf{k}_i \cdot \mathbf{r}} \quad (82)$$

whereas, if $\mathbf{k}_{i\perp} = \mathbf{0}$, we obtain

$$\mathbf{E}_{TE} = \mathbf{e}_{TEM} e^{-j\mathbf{k}_i \cdot \mathbf{r}} \quad (83)$$

$$\mathbf{H}_{TE} = \frac{-k_{iz}}{\omega\mu} \mathbf{e}_{TEM} \times \mathbf{u}_z e^{-j\mathbf{k}_i \cdot \mathbf{r}} \quad (84)$$

and, of course,

$$\mathbf{E}_{TM} = \mathbf{0} \text{ and } \mathbf{H}_{TM} = \mathbf{0}. \quad (85)$$

For any value of \mathbf{k}_i , we have

$$\mathbf{E}_{TE} \cdot \mathbf{k}_i = 0 \text{ and } \mathbf{H}_{TE} = \frac{\mathbf{k}_i}{\omega\mu} \times \mathbf{E}_{TE} \quad (86)$$

and

$$\mathbf{E}_{TM} \cdot \mathbf{k}_i = 0 \text{ and } \mathbf{H}_{TM} = \frac{\mathbf{k}_i}{\omega\mu} \times \mathbf{E}_{TM} \quad (87)$$

so that \mathcal{F}_{TE} , \mathcal{F}_{TM} , and \mathcal{F}_i are TEM to \mathbf{k}_i . This does not entail an orthogonality of \mathbf{E}_{TE} , \mathbf{H}_{TE} , \mathbf{E}_{TM} , or \mathbf{H}_{TM} to the direction of propagation, except in the case where \mathbf{k}_i is real, or, more generally, in the case where \mathbf{k}_i is collinear to its real part.

According to (79)–(85), \mathcal{F}_{TE} and \mathcal{F}_{TM} are plane waves of wave vector \mathbf{k}_i , like \mathcal{F}_i . In contrast, \mathcal{F}_A , \mathcal{F}_B , \mathcal{F}_C , and \mathcal{F}_D are not plane waves, since, according to Section III, each of them is a linear combination of the incident plane wave of wave vector \mathbf{k}_i and a plane wave of wave vector \mathbf{k}_m given by

$$\mathbf{k}_m = \mathbf{k}_i - 2(\mathbf{k}_i \cdot \mathbf{u}_z)\mathbf{u}_z = k_{ix}\mathbf{u}_x + k_{iy}\mathbf{u}_y - k_{iz}\mathbf{u}_z. \quad (88)$$

Fig. 4 shows the planar loop antenna of Fig. 1(c) lying in the plane $z = 0$, the real part $\beta_i = \text{Re}(\mathbf{k}_i)$ of the wave vector

\mathbf{k}_i , and the real part $\beta_m = \text{Re}(\mathbf{k}_m)$ of the wave vector \mathbf{k}_m . The values of \mathcal{F}_A , \mathcal{F}_B , \mathcal{F}_C , and \mathcal{F}_D everywhere in space are provided in the Appendix. Using (57)–(64) and (77)–(78), or, alternatively, the results of the Appendix, we obtain, in the plane $z = 0$,

$$\mathbf{E}_A = \begin{cases} \mathbf{e}_{TEM} e^{-j\mathbf{k}_i \cdot \mathbf{r}}, & \text{if } \mathbf{k}_{i\perp} = \mathbf{0} \\ jv_{TE} \mathbf{k}_{i\perp} \times \mathbf{u}_z e^{-j\mathbf{k}_i \cdot \mathbf{r}}, & \text{if } \mathbf{k}_{i\perp} \neq \mathbf{0} \end{cases} \quad (89)$$

$$\mathbf{H}_A = \frac{v_{TE}}{j\omega\mu} (\mathbf{k}_{i\perp} \cdot \mathbf{k}_{i\perp}) \mathbf{u}_z e^{-j\mathbf{k}_i \cdot \mathbf{r}} \quad (90)$$

$$\mathbf{E}_B = \frac{-i_{TM}}{j\omega\epsilon} k_{iz} \mathbf{k}_{i\perp} e^{-j\mathbf{k}_i \cdot \mathbf{r}} \quad (91)$$

$$\mathbf{H}_C = \begin{cases} \frac{k_{iz}}{\omega\mu} \mathbf{u}_z \times \mathbf{e}_{TEM} e^{-j\mathbf{k}_i \cdot \mathbf{r}}, & \text{if } \mathbf{k}_{i\perp} = \mathbf{0} \\ \frac{-v_{TE}}{j\omega\mu} k_{iz} \mathbf{k}_{i\perp} e^{-j\mathbf{k}_i \cdot \mathbf{r}}, & \text{if } \mathbf{k}_{i\perp} \neq \mathbf{0} \end{cases} \quad (92)$$

$$\mathbf{E}_D = \frac{i_{TM}}{j\omega\epsilon} (\mathbf{k}_{i\perp} \cdot \mathbf{k}_{i\perp}) \mathbf{u}_z e^{-j\mathbf{k}_i \cdot \mathbf{r}} \quad (93)$$

and

$$\mathbf{H}_D = -ji_{TM} \mathbf{k}_{i\perp} \times \mathbf{u}_z e^{-j\mathbf{k}_i \cdot \mathbf{r}} \quad (94)$$

which, combined with (60)–(61), completely define the ETHEFs.

Let \mathbf{E}_{i0} be \mathbf{E}_i at the origin, and \mathbf{H}_{i0} be \mathbf{H}_i at the origin. We observe that, based on (21) and (79)–(84), or on (56) and (89)–(94), if $\mathbf{k}_{i\perp} = \mathbf{0}$,

$$\mathbf{e}_{TEM} = \mathbf{E}_{i0} \quad (95)$$

whereas, if $\mathbf{k}_{i\perp} \neq \mathbf{0}$,

$$v_{TE} = -j \frac{\mathbf{E}_{i0} \cdot (\mathbf{k}_{i\perp} \times \mathbf{u}_z)}{\mathbf{k}_{i\perp} \cdot \mathbf{k}_{i\perp}} \quad (96)$$

and

$$i_{TM} = j \frac{\mathbf{H}_{i0} \cdot (\mathbf{k}_{i\perp} \times \mathbf{u}_z)}{\mathbf{k}_{i\perp} \cdot \mathbf{k}_{i\perp}}. \quad (97)$$

Thus, since $\mathbf{H}_{i0} = \mathbf{k}_i \times \mathbf{E}_{i0}/(\omega\mu)$, we find that the knowledge of \mathbf{k}_i and \mathbf{E}_{i0} is sufficient to directly determine the ETHEFs in the plane $z = 0$, using (89)–(97).

VI. SOME OTHER PARTICULAR INCIDENT FIELDS

A. Superposition of Plane Waves

It might be convenient to represent \mathcal{F}_i as a superposition of time-harmonic plane waves. For instance, this superposition may consist of a primary plane wave and its reflection on a conducting plane, or of an integral of plane waves providing a plane-wave spectrum representation [20, Sec. 19.2], [21].

The results of Section V are applicable to any complex \mathbf{k}_i satisfying (76), so that all possible uniform plane waves and evanescent plane waves are included. It follows that, if \mathcal{F}_i is a known superposition of time-harmonic plane waves, it is possible to apply the results of Section V to each of them. Thus, \mathcal{F}_A is obtained as a superposition of electromagnetic fields each given by (89)–(90) applied to one of the time-harmonic plane waves, \mathcal{F}_B is obtained as a superposition of electromagnetic fields each given by (60) and (91) applied to one of the time-harmonic plane waves, etc.

B. Magnetic Dipole Normal to the Plane $z = 0$

The electric field produced by a magnetic dipole of moment $\mathbf{m} = m\mathbf{u}_z$ lying at the origin is [20, Sec 15.5] [22, Sec 8.6]

$$\begin{aligned} \mathbf{E} &= \frac{-k^2\eta}{4\pi r} \left(1 + \frac{1}{jkr}\right) \mathbf{u}_r \times \mathbf{m} e^{-jkr} \\ &= \frac{k^2m\eta}{4\pi r} \left(1 + \frac{1}{jkr}\right) \sin\theta \mathbf{u}_\varphi e^{-jkr} \end{aligned} \quad (98)$$

where $\eta = (\mu/\epsilon)^{1/2}$, and where r , θ , and φ are the usual spherical coordinates of the observation point, the unitary vectors of the spherical coordinates being denoted by \mathbf{u}_r , \mathbf{u}_θ and \mathbf{u}_φ .

We now consider the electromagnetic field \mathcal{F}_i produced by a magnetic dipole of moment $\mathbf{m} = m\mathbf{u}_z$ lying at $x = x_S$, $y = y_S$ and $z = z_S$. By (98), this spherical wave is such that

$$\mathbf{E}_i = \frac{k^2m\eta}{4\pi D^2} \left(1 + \frac{1}{jkD}\right) [-(y-y_S)\mathbf{u}_x + (x-x_S)\mathbf{u}_y] e^{-jkD} \quad (99)$$

where

$$D = \sqrt{(x-x_S)^2 + (y-y_S)^2 + (z-z_S)^2} \quad (100)$$

Thus, \mathcal{F}_i produced by the magnetic dipole is TE to z , so that we may write $\mathcal{F}_i = \mathcal{F}_{TE}$. Consequently, by the definition of the ETHEFs, we have, in the plane $z = 0$,

$$\mathbf{E}_A = \mathbf{E}_i \quad (101)$$

and

$$\mathbf{E}_B = \mathbf{0} \quad (102)$$

which, combined with (65) are sufficient to determine the different contributions in (72) or (73), if \mathbf{E}_i and \mathbf{H}_i are known.

C. Circular Loop Parallel to the Plane $z = 0$

As said in the introduction, a possible calibration technique for a field-strength meter is the standard-field method, in which the circular loop antenna of the field-strength meter to be calibrated is excited by a coaxial single-turn circular transmitting loop antenna [5]. For instance, the National Bureau of Standards (NBS) used a transmitting loop of radius $b = 10$ cm, up to 50 MHz, the distance d between the planes of the transmitting loop antenna and of the field-strength meter's loop antenna ranging from 1.5 m to 3 m [23]. The calibration was based on the "formula of Greene", that is formula (24) of [24], which takes propagation between the loops into account, but which assumes a uniform current in the transmitting loop, because the radius b of the transmitting loop antenna is (assumed to be) sufficiently small.

We therefore consider the electromagnetic field \mathcal{F}_i produced by a circular loop antenna, in which a practically uniform current flows, the loop antenna being parallel to the plane $z = 0$, its center lying at $x = x_S$, $y = y_S$, and $z = z_S$. In this case, \mathbf{E}_i is everywhere (practically) parallel to the plane $z = 0$ and may be written in the form of an involved analytic formula [25]–[32]. Thus, \mathcal{F}_i produced by the circular loop antenna

is (practically) TE to z , so that we may write $\mathcal{F}_i \approx \mathcal{F}_{TE}$. Consequently, we have, in the plane $z = 0$,

$$\mathbf{E}_A \approx \mathbf{E}_i \quad (103)$$

and

$$\mathbf{E}_B \approx \mathbf{0} \quad (104)$$

which, combined with (65), are sufficient to approximately determine the different contributions in (72) or (73), if \mathbf{E}_i and \mathbf{H}_i are known.

We see that the effects of \mathcal{F}_B are completely ignored in the calibration technique described above, so that the resulting accuracy of the field-strength meter might be questioned.

D. Short Discussion

If we know \mathcal{F}_i , we have identified 3 ways of computing \mathcal{F}_A and \mathcal{F}_B in the plane $z = 0$, in order to be able to use (72) or (73). The first approach relies on solving the scalar partial differential equations (22)–(23) to obtain ψ_{TE} and ψ_{TM} , deriving \mathcal{F}_{TE} and \mathcal{F}_{TM} , and using the definition of the ETHEFs, set out in Section III-B. The second approach, presented in Section V or Section VI-A, is applicable if \mathcal{F}_i is a known plane wave (which need not be a uniform plane wave) or a superposition of known plane waves. The third approach, exemplified in Sections VI-B and VI-C, applies to particular forms of \mathcal{F}_i .

VII. CONCLUSION

We have presented and used a new and specialized decomposition of an arbitrary incident time-harmonic electromagnetic field \mathcal{F}_i into the ETHEFs \mathcal{F}_A , \mathcal{F}_B , \mathcal{F}_C and \mathcal{F}_D , which are shown to be useful to study the response of an arbitrary planar wire loop antenna used for reception.

We have obtained a formula (72) which gives the response of the arbitrary planar wire loop antenna receiving \mathcal{F}_i . This formula is applicable to any incident field configuration and valid at any frequency at which the thin wire approximation applies. It separates the response of the antenna into three parts: a surface integral of \mathbf{H}_A , a line integral of \mathbf{E}_A , and a line integral of \mathbf{E}_B . This decomposition shows that, at any frequency, only \mathcal{F}_A and \mathcal{F}_B excite the antenna.

It is possible, especially at low frequencies, to consider that \mathcal{F}_A causes the intended response of the antenna, while \mathcal{F}_B may cause an unwanted response. In (72) the effect \mathcal{F}_A is subdivided into the surface integral of \mathbf{H}_A , which may be viewed as the intended response of the antenna, and the line integral of \mathbf{E}_A , which can be viewed as a correction term for the gap width and the nonuniformity of the high-frequency current distribution, since this line integral vanishes if the current is uniform over the integration path.

This paper is directed at a planar wire loop antenna used as a measuring antenna or as a direction finder. It was recognized a long time ago that, if the antenna is not very small (e.g., a circular loop antenna of diameter less than 0.01λ , if \mathcal{F}_i is a uniform plane wave [1]), the goal “measuring a magnetic component of \mathcal{F}_i ”, used in the introduction section, is not consistent with the actual capabilities of the loop antenna. This

paper teaches that, up to larger antenna sizes, a reasonable purpose of the measurement is to obtain information about \mathcal{F}_A , in the presence of unwanted effects of \mathcal{F}_B (and possibly of \mathcal{F}_C or \mathcal{F}_D , since an actual antenna is different from the theoretical planar wire antenna that we have assumed).

If we except calibration procedures, little information about \mathcal{F}_i is typically available before a measurement, so that the question of computing \mathcal{F}_A and \mathcal{F}_B does not arise. In contrast, in the context of a calibration operation during which the planar wire loop antenna is used for reception, a computation of \mathcal{F}_A and \mathcal{F}_B is possible and useful to analyze the calibration.

APPENDIX

Using (26)–(33), (79)–(85), and (88), we find that, in the case of an incident plane wave, \mathcal{F}_A , \mathcal{F}_B , \mathcal{F}_C , and \mathcal{F}_D everywhere in space are, if $\mathbf{k}_{i\perp} \neq \mathbf{0}$, given by

$$\mathbf{E}_A = jv_{TE} \mathbf{k}_{i\perp} \times \mathbf{u}_z \frac{e^{-j\mathbf{k}_i \cdot \mathbf{r}} + e^{-j\mathbf{k}_m \cdot \mathbf{r}}}{2} \quad (105)$$

$$\mathbf{H}_A = \frac{v_{TE}}{2j\omega\mu} ([(\mathbf{k}_{i\perp} \cdot \mathbf{k}_{i\perp})\mathbf{u}_z - k_{iz}\mathbf{k}_{i\perp}] e^{-j\mathbf{k}_i \cdot \mathbf{r}} + [(\mathbf{k}_{i\perp} \cdot \mathbf{k}_{i\perp})\mathbf{u}_z + k_{iz}\mathbf{k}_{i\perp}] e^{-j\mathbf{k}_m \cdot \mathbf{r}}) \quad (106)$$

$$\mathbf{E}_B = \frac{i_{TM}}{2j\omega\epsilon} ([(\mathbf{k}_{i\perp} \cdot \mathbf{k}_{i\perp})\mathbf{u}_z - k_{iz}\mathbf{k}_{i\perp}] e^{-j\mathbf{k}_i \cdot \mathbf{r}} - [(\mathbf{k}_{i\perp} \cdot \mathbf{k}_{i\perp})\mathbf{u}_z + k_{iz}\mathbf{k}_{i\perp}] e^{-j\mathbf{k}_m \cdot \mathbf{r}}) \quad (107)$$

$$\mathbf{H}_B = -ji_{TM} \mathbf{k}_{i\perp} \times \mathbf{u}_z \frac{e^{-j\mathbf{k}_i \cdot \mathbf{r}} - e^{-j\mathbf{k}_m \cdot \mathbf{r}}}{2} \quad (108)$$

$$\mathbf{E}_C = jv_{TE} \mathbf{k}_{i\perp} \times \mathbf{u}_z \frac{e^{-j\mathbf{k}_i \cdot \mathbf{r}} - e^{-j\mathbf{k}_m \cdot \mathbf{r}}}{2} \quad (109)$$

$$\mathbf{H}_C = \frac{v_{TE}}{2j\omega\mu} ([(\mathbf{k}_{i\perp} \cdot \mathbf{k}_{i\perp})\mathbf{u}_z - k_{iz}\mathbf{k}_{i\perp}] e^{-j\mathbf{k}_i \cdot \mathbf{r}} - [(\mathbf{k}_{i\perp} \cdot \mathbf{k}_{i\perp})\mathbf{u}_z + k_{iz}\mathbf{k}_{i\perp}] e^{-j\mathbf{k}_m \cdot \mathbf{r}}) \quad (110)$$

$$\mathbf{E}_D = \frac{i_{TM}}{2j\omega\epsilon} ([(\mathbf{k}_{i\perp} \cdot \mathbf{k}_{i\perp})\mathbf{u}_z - k_{iz}\mathbf{k}_{i\perp}] e^{-j\mathbf{k}_i \cdot \mathbf{r}} + [(\mathbf{k}_{i\perp} \cdot \mathbf{k}_{i\perp})\mathbf{u}_z + k_{iz}\mathbf{k}_{i\perp}] e^{-j\mathbf{k}_m \cdot \mathbf{r}}) \quad (111)$$

and

$$\mathbf{H}_D = -ji_{TM} \mathbf{k}_{i\perp} \times \mathbf{u}_z \frac{e^{-j\mathbf{k}_i \cdot \mathbf{r}} + e^{-j\mathbf{k}_m \cdot \mathbf{r}}}{2} \quad (112)$$

whereas, if $\mathbf{k}_{i\perp} = \mathbf{0}$, we obtain

$$\mathbf{E}_A = \mathbf{e}_{TEM} \frac{e^{-j\mathbf{k}_i \cdot \mathbf{r}} + e^{-j\mathbf{k}_m \cdot \mathbf{r}}}{2} \quad (113)$$

$$\mathbf{H}_A = \frac{-k_{iz}}{\omega\mu} \mathbf{e}_{TEM} \times \mathbf{u}_z \frac{e^{-j\mathbf{k}_i \cdot \mathbf{r}} - e^{-j\mathbf{k}_m \cdot \mathbf{r}}}{2} \quad (114)$$

$$\mathbf{E}_B = \mathbf{0} \text{ and } \mathbf{H}_B = \mathbf{0} \quad (115)$$

$$\mathbf{E}_C = \mathbf{e}_{TEM} \frac{e^{-j\mathbf{k}_i \cdot \mathbf{r}} - e^{-j\mathbf{k}_m \cdot \mathbf{r}}}{2} \quad (116)$$

$$\mathbf{H}_C = \frac{-k_{iz}}{\omega\mu} \mathbf{e}_{TEM} \times \mathbf{u}_z \frac{e^{-j\mathbf{k}_i \cdot \mathbf{r}} + e^{-j\mathbf{k}_m \cdot \mathbf{r}}}{2} \quad (117)$$

and

$$\mathbf{E}_D = \mathbf{0} \text{ and } \mathbf{H}_D = \mathbf{0}. \quad (118)$$

REFERENCES

- [1] H. Whiteside and R. W. P. King, "The loop antenna as a probe," *IEEE Trans. Antennas Propag.*, vol. AP-12, no. 3, pp. 291–297, May 1964.
- [2] G. S. Smith, "Loop antennas," in *Antenna Engineering Handbook*, R. C. Johnson, Ed., 3rd ed. New York, NY, USA: McGraw-Hill, 1993, ch. 5.
- [3] R. W. P. King, "The loop antenna for transmission and reception" in *Antenna Theory, Part I*. R. E. Collin and F. J. Zucker, Eds. New York, NY, USA: McGraw-Hill, 1969, ch. 11.
- [4] F. E. Terman, *Radio Engineers' Handbook*. New York, NY, USA: McGraw-Hill, 1943.
- [5] F. M. Greene, "NBS field-strength standards and measurements (30 Hz to 1000 MHz)," *Proc. IEEE*, vol. 55, no. 6, pp. 970–981, Jun. 1967.
- [6] *C.I.S.P.R. Publication 16, C.I.S.P.R. Specification for Radio Interference Measuring Apparatus and Measurement Methods*, Bureau Central de la Commission Electrotechnique Internationale, 1977.
- [7] *HF Field-Strength Measurement*, Recommendation ITU-R P.845-3, 1997.
- [8] *Specification for Radio Disturbance and Immunity Measuring Apparatus and Methods—Part 1: Radio Disturbance and Immunity Measuring Apparatus*. CISPR 16-1 (1999-10), International Electrotechnical Commission, 1999.
- [9] *Field-Strength Measurements at Monitoring Stations*, Recommendation ITU-R SM.378-7, ITU, 2007.
- [10] *Handbook Spectrum Monitoring*, ITU, Geneva, Switzerland, 2011.
- [11] *Specification for Radio Disturbance and Immunity Measuring Apparatus and Methods—Part 1-4: Radio Disturbance and Immunity Measuring Apparatus—Antennas and Test Sites for Radiated Disturbance Measurements*, CISPR 16-1-4 (2019-01), IEC, 2019.
- [12] H. D. Kennedy and R. B. Woolsey, "Direction-finding antennas," in *Antenna Engineering Handbook*, R. C. Johnson, Ed., 3rd ed., New York, NY, USA: McGraw-Hill, 1993, ch. 39.
- [13] Y. Tian, B. Wen, J. Tan, and Z. Li, "Study on pattern distortion and DOA estimation performance of crossed-loop/monopole antenna in HF radar," *IEEE Trans. Antennas Propag.*, vol. 65, no. 11, pp. 6095–6106, Nov. 2017.
- [14] S. Khan, K. T. Wong, Y. Song, and W.-Y. Tam, "Electrically large circular loops in the estimation of an incident emitter's direction-of-arrival or polarization," *IEEE Trans. Antennas Propag.*, vol. 66, no. 6, pp. 3046–3055, Jun. 2018.
- [15] E. C. Jordan and K. G. Balmain, *Electromagnetic Waves and Radiating Systems*, 2nd ed. Englewood Cliffs, NJ, USA: Prentice-Hall, 1968.
- [16] P. M. Morse and H. Feshbach, *Methods of Theoretical Physics, Part II*, New York, NY, USA: McGraw-Hill, 1953.
- [17] R. F. Harrington, *Time-Harmonic Electromagnetic Fields*. New York, NY, USA: McGraw-Hill, 1961.
- [18] S. A. Schelkunoff, *Electromagnetic Waves*. New York, NY, USA: Van Nostrand, 1943.
- [19] J. D. Jackson, *Classical Electrodynamics*, 2nd ed. New York, NY, USA: Wiley, 1975.
- [20] S. J. Orfanidis, *Electromagnetic Waves and Antennas*, vol. 2. Sophocles J. Orfanidis, 2016.
- [21] P. C. Clemmow, *The Plane Wave Spectrum Representation of Electromagnetic Fields*. Oxford, U.K.: Pergamon Press, 1966.
- [22] J. A. Stratton, *Electromagnetic Theory*. New York, NY, USA: McGraw-Hill, 1941.
- [23] M. Kanda, E. B. Larsen, M. Borsero, P. G. Galliano, I. Yokoshima, and N. S. Nahman, "Standards for electromagnetic field measurements," *Proc. IEEE*, vol. 74, no. 1, pp. 120–128, Jan. 1986.
- [24] F. M. Greene, "The near-zone magnetic field of a small circular-loop antenna," *J. Res. Nat. Bur. Standards C, Eng. Inst.*, vol. 71C, no. 4, pp. 319–326, Oct. 1967.
- [25] D. H. Werner, "An exact integration procedure for vector potentials of thin circular loop antennas," *IEEE Trans. Antennas Propag.*, vol. 44, no. 2, pp. 157–165, Feb. 1996.
- [26] P. L. Overfelt, "Near fields of the constant current thin circular loop antenna of arbitrary radius," *IEEE Trans. Antennas Propag.*, vol. 44, no. 2, pp. 166–171, Feb. 1996.
- [27] L.-W. Li, M.-S. Leong, P.-S. Kooi, and T.-S. Yeo, "Exact solutions of electromagnetic fields in both near and far zones radiated by thin circular-loop antennas: A general representation," *IEEE Trans. Antennas Propag.*, vol. 45, no. 12, pp. 1741–1748, Dec. 1997.
- [28] D. H. Werner *et al.*, "Comments on 'Exact solutions of electromagnetic fields in both near and far zones radiated by thin circular-loop antennas: A general representation,'" *IEEE Trans. Antennas Propag.*, vol. 49, no. 1, pp. 109–110, Jan. 2001.
- [29] J. T. Conway, "New exact solution procedure for the near fields of the general thin circular loop antenna," *IEEE Trans. Antennas Propag.*, vol. 53, no. 1, pp. 509–517, Jan. 2005.
- [30] S. M. A. Hamed, "Exact field expressions for circular loop antennas using spherical functions expansion," *IEEE Trans. Antennas Propag.*, vol. 61, no. 6, pp. 2956–2963, Jun. 2013.
- [31] K. H. R. Zheng, J. L.-W. Li, and S. M. A. Hamed, "Comments on 'Exact field expressions for circular loop antennas using spherical functions expansion,'" *IEEE Trans. Antennas Propag.*, vol. 62, no. 8, pp. 4432–4434, Aug. 2014.
- [32] S. M. A. Hamed, "Response to 'Comments on 'Exact field expressions for circular loop antennas using spherical functions expansion,'" *IEEE Trans. Antennas Propag.*, vol. 62, no. 8, p. 4434, Aug. 2014.



Frédéric Broydé (S'84–M'86–SM'01) was born in France in 1960. He received the M.S. degree in physics engineering from the Ecole Nationale Supérieure d'Ingénieurs Electriciens de Grenoble (ENSIEG) and the Ph.D. in microwaves and microtechnologies from the Université des Sciences et Technologies de Lille (USTL).

He co-founded the Excem corporation in May 1988, a company providing engineering and research and development services. He is president and CTO of Excem. Most of his activity is allocated to engineering and research in electronics. Currently, his most active research areas is wireless transmission systems, with an emphasis on antenna tuning.

Dr. Broydé is author or co-author of about 100 technical papers, and inventor or co-inventor of about 80 patent families, for which more than 45 US patents have been granted. He is a licensed radio amateur (F5OYE).



Evelyne Clavelier (S'84–M'85–SM'02) was born in France in 1961. She received the M.S. degree in physics engineering from the Ecole Nationale Supérieure d'Ingénieurs Electriciens de Grenoble (ENSIEG).

She is co-founder of the Excem corporation, based in Maule, France. She is CEO of Excem. She is also manager of Eurexcm (a subsidiary of Excem) and President of Tekcem, a company selling or licensing intellectual property rights. She is also an active engineer and researcher. Her current research area is radio communications. She has also done research work in the areas of electromagnetic compatibility (EMC) and signal integrity. She has taken part in many electronic design and software design projects of Excem.

Prior to starting Excem in 1988, she worked for Schneider Electric (in Grenoble, France), STMicroelectronics (in Grenoble, France), and Signetics (in Mountain View, USA).

Ms. Clavelier is the author or a co-author of about 80 technical papers. She is co-inventor of more about 80 patent families. She is a licensed radio amateur (F1PHQ).